



The Abdus Salam
International Centre for Theoretical Physics



1856-49

2007 Summer College on Plasma Physics

30 July - 24 August 2007

**Properties of drift and Alfvén waves
in collisional plasmas.**

VRANJES Jovo

K.U. Leuven
Centre for Plasma Astrophysics
Celestijnenlaan 200 B
3001 Heverlee, Leuven
Belgium

Properties of drift and Alfvén waves

in collisional plasmas

J. Vranjes

Center for Plasma Astrophysics, Celestijnenlaan 200B, 3001 Leuven, Belgium

and

Faculté des Sciences Appliquées, avenue F.D. Roosevelt 50, 1050 Bruxelles, Belgium

Permanent affiliation: Institute of Physics, Belgrade, Yugoslavia \Rightarrow Serbia and Montenegro \Rightarrow Serbia

In collaboration with: [S. Poedts](#)¹, [B. P. Pandey](#)², [B. De Pontieu](#)³

¹ *Center for Plasma Astrophysics, Celestijnenlaan 200B, 3001 Leuven, Belgium*

² *Department of Physics, Macquarie University, Sydney, NSW 2109, Australia*

³ *Lockheed Martin Solar and Astrophysics Lab, 3251 Hanover St., Org. ADBS, Bldg. 252, Palo Alto, CA 94304,*

USA

Plan

1. Motivation
2. Alfvén wave in strongly collisional plasmas
 - physical picture
 - wave energy flux
3. Drift-Alfvén wave in collisional plasmas
 - hot ions effects
 - local and global modes

1. Motivation

Academic:

- to try to understand the physics of waves in collision dominated/weakly ionized plasmas
- investigate the effects of neutrals

- Apply the results to solar atmosphere

Reasons for applying to solar atmosphere:

a) The convective motions (typical velocities about 0.5 km/s; values up to 2 km/s also possible) in the solar photosphere, resulting in the foot point motion of different magnetic structures in the solar atmosphere, are frequently proposed as the source for the excitation of Alfvén waves, which are assumed to propagate towards the chromosphere and corona resulting finally in the heating of these layers by the dissipation of this wave energy. However, the photosphere is i) very weakly ionized, and, ii) the dynamics of the plasma particles in this region is heavily influenced by the plasma-neutral collisions. The purpose of this work is to check the consequences of these two facts on the above scenario and their effects on the electromagnetic waves.

b) Solar plasmas are structured and stratified both vertically and horizontally. The presence of density gradients and magnetic fields results in an additional wave which can be electrostatic (the drift wave) and electromagnetic (the drift-Alfvén wave), and can not be predicted in the widely used MHD description.

2. Alfvén wave in strongly collisional plasmas

On collisions in weakly ionized plasmas

- We introduce here the collision frequencies between charged and uncharged particles $\nu_{jn} = n_{n0}\sigma_{jn}v_{Tj}$ for $j = e, i$, and the Spitzer-Härm formulas¹ for the Coulomb collisions between charged plasma particles:

$$\nu_{ee} + \nu_{ei} \simeq 2\nu_{ei} = \left[4n_{e0}(2\pi/m_e)^{1/2} [ee_i/(4\pi\epsilon_0)]^2 L_{ei} / [3(\kappa T_e)^{3/2}] \right],$$

$$\nu_{ii} = \left[4n_{i0}(\pi/m_i)^{1/2} [e_i^2/(4\pi\epsilon_0)]^2 L_{ii} / [3(\kappa T_i)^{3/2}] \right].$$

The Coulomb logarithm $L_{ei} = \log[12\pi\epsilon_0(\epsilon_0/n_{i0})^{1/2}(\kappa T_e)^{3/2}/(ee_i^2)]$.

- Several comments.

- Using the full quantum theory as well as the semi-classical approach, the elastic proton-hydrogen ($H^+ + H$) collision cross section is calculated by Krstic and

¹L. Spitzer, Physics of Fully Ionized Gasses (Interscience Publishers, New York-London, 1962) p. 146

Schultz², and its integral value at 0.5 eV is about $1.8 \cdot 10^{-18} \text{ m}^2$ for the elastic scattering, and about 10^{-18} m^2 for the momentum transfer. As for the electron-hydrogen ($e^- + H$) collisions, the collision cross section is also temperature dependent and the corresponding values can be found in the work of Bedersen and Kieffer³. At energies of 0.5 eV it is about $3.5 \cdot 10^{-19} \text{ m}^2$, so that for the elastic scattering we have $\sigma_{in}/\sigma_{en} \simeq 6$.

- We do not include the inelastic collisions which take place in a partially ionized plasma like in the photosphere. It can be shown⁴ that, in the photosphere, all ions in a unit volume are recombined many times per second. The three-body recombination (the process of the type $H^+ + e^- + e^- \rightarrow H + e^-$) is dominant in this region. At the altitude of $h = 500 \text{ km}$, the radiative recombination (the process described by $H^+ + e^- \rightarrow H + h\nu$) and the three-body recombination are of the same order. At higher altitudes the radiative recombination becomes the leading loss effect. At $h = 1000 \text{ km}$ it is by a factor 100 larger than the three-body

²P. S. Krstic and D. R. Schultz, J. Phys. B: At. Mol. Opt. Phys. **32**, 3485 (1999)

³B. Bedersen and L. J. Kieffer, Rev. Mod. Phys. **43**, 601 (1971)

⁴J. Vranjes and S. Poedts, Phys. Lett. A **348**, 346 (2008)

recombination.

- Also, the charge exchange between the ionized and neutral hydrogen is frequent. The cross section for the proton-hydrogen charge exchange σ_{ex} at the above given temperatures is about $5.6 \cdot 10^{-19} \text{ m}^2$, i.e., for hydrogen it is a large fraction ($\simeq 0.3$) of the realistic elastic scattering cross section σ_{in} given above. Note, however, that for some other gases like He, Ne, and Ar, we have $\sigma_{ex} > \sigma_{in}$ the charge exchange cross section exceeds the one for the elastic scattering⁵
- Consequently, due to the inelastic collisions and the charge exchange, neutrals/ions in the plasma spend a part of their time in the ionized/neutral state, respectively. As a result, the effective collision frequencies are expected to be even higher than the values which we shall use.

Physical picture of the Alfvén wave

- In the case of the shear Alfvén wave with $\vec{B}_0 = B_0 \vec{e}_z$, both ion and electron fluids oscillate in the direction of the perturbed magnetic field vector $\vec{B}_1 = B_1 \vec{e}_y$. This is due to the $\vec{E}_1 \times \vec{B}_0$ drift, which does not separate neither charges nor masses,

⁵Y. P. Raizer, Gas discharge physics (Springer-Verlag, Berlin Heidelberg, 1991), p. 25.

and the direction of the electric field is determined by the Faraday law. The wave is sustained by the additional polarization drift $\vec{v}_{pj} = (m_j/q_j B_0^2) \partial \vec{E}_1 / \partial t$ and the consequent Lorentz force $j_x \vec{e}_x \times \vec{B}_0$ which is in the y -direction and has a proper phase shift. The polarization drift introduces the ion inertia effects and if it is neglected, then the Alfvén wave vanishes. The $\vec{E} \times \vec{B}$ term essentially describes the magnetic field frozen-in property of the plasma.

- The mode fully described by the wave equation

$$\nabla \times \nabla \times \vec{E}_1 = \frac{\omega^2}{c^2} \vec{E}_1 + \frac{i\omega}{\varepsilon_0 c^2} \vec{j}_1, \quad (1.1)$$

the momentum equations for ions and electrons

$$m_i n_i \left[\frac{\partial \vec{v}_i}{\partial t} + (\vec{v}_i \cdot \nabla) \vec{v}_i \right] = e n_i \left(\vec{E} + \vec{v}_i \times \vec{B} \right) - m_i n_i \nu_{in} (\vec{v}_i - \vec{v}_n) - m_i n_i \nu_{ie} (\vec{v}_i - \vec{v}_e), \quad (1.2)$$

$$m_e n_e \left[\frac{\partial \vec{v}_e}{\partial t} + (\vec{v}_e \cdot \nabla) \vec{v}_e \right] = -e n_e \left(\vec{E} + \vec{v}_e \times \vec{B} \right) - m_e n_e \nu_{en} (\vec{v}_e - \vec{v}_n) - m_e n_e \nu_{ei} (\vec{v}_e - \vec{v}_i), \quad (1.3)$$

and the corresponding [equation for neutrals](#)

$$m_n n_n \left[\frac{\partial \vec{v}_n}{\partial t} + (\vec{v}_n \cdot \nabla) \vec{v}_n \right] = -m_n n_n \nu_{ni} (\vec{v}_n - \vec{v}_i) - m_n n_n \nu_{ne} (\vec{v}_n - \vec{v}_e). \quad (1.4)$$

- [Without collisions](#) the energy flux of the Alfvén wave

$$F_{id} = m_i n_0 v_i^2 c_a / 2. \quad (1.5)$$

$v_i = E_1 / B_0$ - the leading order $\vec{E} \times \vec{B}$ perturbed ion velocity. Using the Faraday law $E_1 = \omega B_1 / k$, hence $v_i = c_a B_1 / B_0$. For the estimate only, we assume small perturbations of the magnetic field, viz. around 1 percent. For the [photosphere](#) at $h = 250$ km, this yields $c_a = B_0 / (\mu_0 n_{i0} m_i) = 1.3 \cdot 10^5$ m/s. Consequently, the perturbed plasma (ion) velocity is $v_i = 10^{-2} c_a = 1.3 \cdot 10^3$ m/s. The wave energy flux in the ideal case, and for $m_i = m_p$, becomes $F_{id} = 5.3 \cdot 10^2$ J/(m²s).

- Collisions may heavily alter the motion of the perturbed electron and ion fluids. The plasma response to the electromagnetic (Alfvén-type) perturbations in fully and weakly ionized plasmas is essentially different from various points of view.
- The collision frequencies (in Hz) and magnetization of electrons and protons in the

photosphere for the magnetic field $B_0 = 10^{-2}$ T.

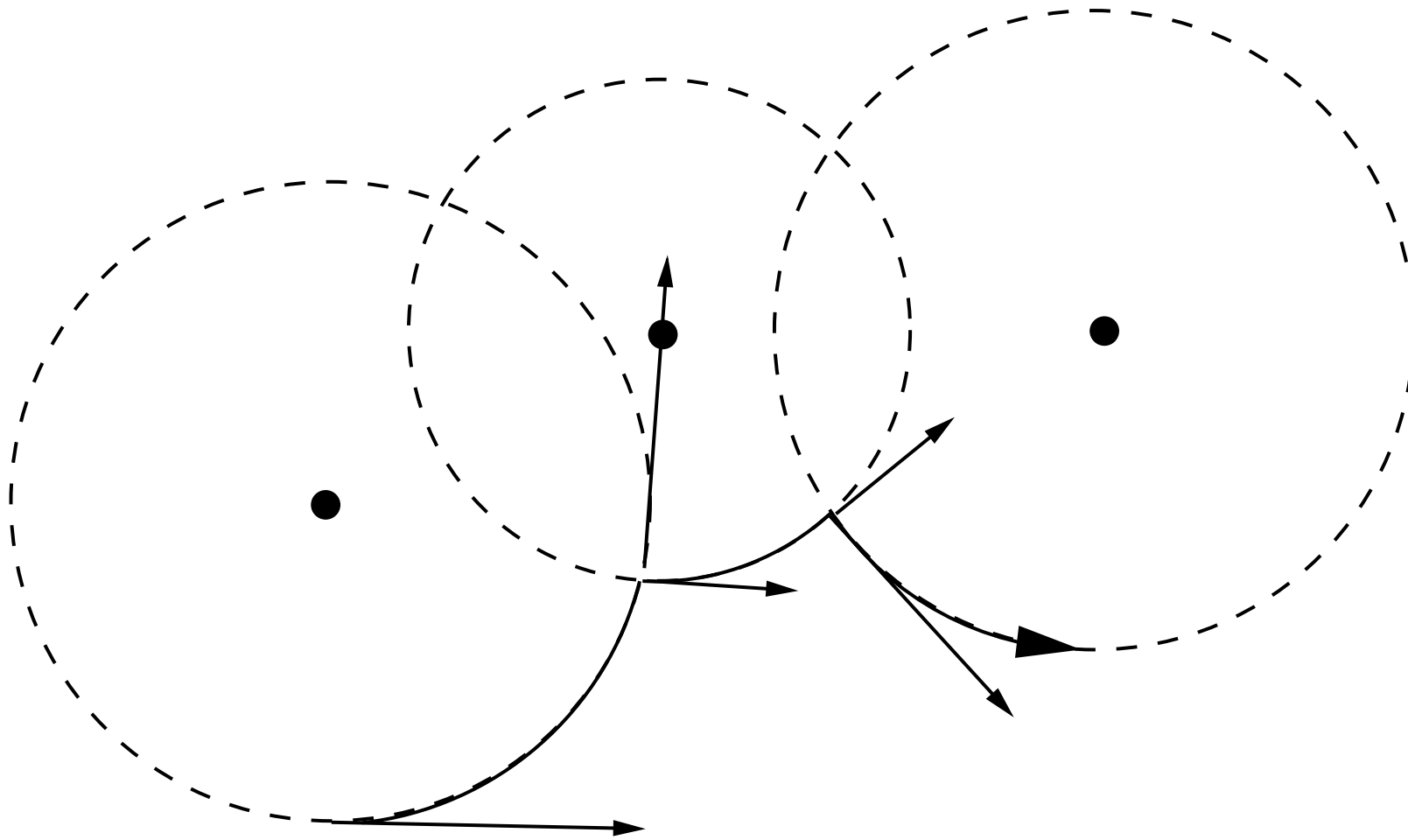
h [km]	ν_{in}	ν_{ii}	ν_{en}	ν_{ei}	Ω_i/ν_{it}	Ω_e/ν_{et}
0	$1.6 \cdot 10^9$	$5 \cdot 10^7$	$1.3 \cdot 10^{10}$	$1.5 \cdot 10^9$	$6 \cdot 10^{-4}$	$1.1 \cdot 10^{-1}$
250	$2.6 \cdot 10^8$	$3.8 \cdot 10^6$	$2.2 \cdot 10^9$	$1.2 \cdot 10^8$	$3.6 \cdot 10^{-3}$	$7.3 \cdot 10^{-1}$

- It is believed that, due to the low temperature, the ions in the lower photosphere are in fact mainly metal ions. Sen and White⁶ have assumed that the mean mass of these metal ions is 35 a.u. In that case, due to the rather different masses of (metal) ions and neutral (hydrogen) atoms, in calculating the collision frequency it is appropriate to use a more accurate formula $\nu_{mn} = n_{n0}\sigma_{mn}[m_n/(m_m+m_n)][8\kappa T_m/(\pi\mu)]^{1/2}$, where the index m denotes the metal ion, n denotes the neutrals (hydrogen), and $\mu = m_m m_n / (m_m + m_n)$ is the reduced mass. Taking the layer $h = 250$ km, we find $\nu_{mm} = 6.4 \cdot 10^5$ Hz, $\nu_{mn} = 4 \cdot 10^8$ Hz, and $\Omega_m = 2.7 \cdot 10^4$ Hz. Comparing to protons the metal ions appear to be even less magnetized, i.e., $\Omega_m/\nu_m = 6.6 \cdot 10^{-5}$, where $\nu_m = \nu_{mm} + \nu_{mn}$. At $h = 0$ km we have $\nu_{mm} = 1.2 \cdot 10^7$ Hz, $\nu_{mn} = 2 \cdot 10^9$ Hz, and $\Omega_m/\nu_m \simeq 1.3 \cdot 10^{-5}$.

⁶H. K. Sen and M. L. White, Sol. Phys., **23**, 146 (1972)

- Some facts:

1. From the ion momentum, the ratio of the Lorentz and the friction forces (for predominant ion-neutral collisions and in the case of initially unperturbed neutrals), is Ω_i/ν_{in} . For the given photospheric plasma this is $\sim 1/10^3$.
 2. Contrary to the case of fully ionized plasma where all particles in a volume element move together due to the given electric field while still colliding with each other, in the present case in the beginning only charged particles move due to the applied electric field, while neutrals have a tendency of staying behind. If $\nu_{in} \gg \Omega_i, \omega$, each plasma particle collides many times within the theoretical gyro-rotation, or within the assumed wave oscillation.
 3. Contrary to the viscosity which is of primary importance for short scale processes, the friction is more effective in the opposite limit, i.e., at smaller wave-numbers (and also at larger wave-periods) an ion is subject to larger number of collisions with neutrals within one oscillation period.
 4. The motion of an un-magnetized charged particle depicted in Fig. 1.1.
-



Figuur 1.1: The motion of a charged particle in non-magnetized plasma. Arrows denote the tangential direction at the moment of collision when the particle switches to another gyro-orbit with a possibly different velocity (indicated by different gyro-radius). A collision occurs after a very tiny fraction (*largely exaggerated here*) of the gyro orbit has been traveled.

Effects of neutrals

- Described in: Kulsrud and Pierce, ApJ **156**, 445 (1969); Pudritz, ApJ **350**, 195 (1990); Haerendel, Nature **360**, 241 (1992); De Pontieu and Harendel, Astron. Astrophys. **338**, 729 (1998); Pécseli and Engvold, Sol. Phys. **194**, 73 (2000).

- a) For a relatively small amount of neutrals (or for short wavelengths) the damping proportional to the collision frequency ν_{in} , **more collisions increases the friction**.
- b) In a weakly ionized plasma the collisions are numerous, the whole fluid moves together. The stronger collisions the better locking of the gas-plasma fluid; the damping of the wave (**proportional to $1/\nu_{in}$**) vanishes.
- c) The Alfvén velocity in such a mixture includes the total fluid density $m_i n_i + m_n n_n$. The dispersion equation [De Pontieu and Haerendel (1998)]:

$$\frac{\omega}{k} = c_A \left(1 - i \frac{m_n n_n}{m_n n_n + m_i n_i} \frac{\omega}{\nu_{ni}} \right)^{1/2}, \quad c_A = \frac{B_0}{[\mu_0 (m_i n_i + m_n n_n)]^{1/2}}.$$

- We suggest the following item to be added in order to complete the physical picture:
 - d) the perturbed velocity of the gas-plasma mixture may be drastically reduced in a weakly ionized plasma and, consequently, **the wave energy flux becomes very small**.

Wave energy flux in strongly collisional plasma- application to photosphere

- Assume the same magnitude of the magnetic field perturbation as in the ideal case discussed above: 1 percent. The perturbed magnetic field \Rightarrow the electric field \Rightarrow the consequent ion motion in the same direction as the perturbed vector \vec{B}_1 . This perturbed $\vec{E} \times \vec{B}$ -drift velocity of ions we denote by V_i . This velocity is the same for electrons, and we are speaking about fluid velocities.
- The relaxation velocity of neutrals and ions can be obtained from the following. Assume that in the starting moment the unit volume of the neutrals have a different velocity V_n . In view of the huge difference in mass we neglect electrons for simplicity. The collision frequency is extraordinary high, of the order of $\sim 10^9$ Hz. Compare this with the theoretical gyro-frequency for ions $\Omega_i \sim 10^6$ Hz. The frequency ordering which we have here is:

$$\omega \ll \Omega_i \ll \nu_i.$$

As a result, we can take the starting/maximal value of the ion velocity V_i and estimate for the value it will take within the collisional time.

- The time dependence of the velocities of the two fluids (ions and neutral) in relative mo-
-

tion is determined by the friction and it can be obtained from the simplified momentum equations:

$$\partial \vec{v}_n / \partial t = \nu_{ni}(\vec{v}_i - \vec{v}_n), \quad \partial \vec{v}_i / \partial t = \nu_{in}(\vec{v}_n - \vec{v}_i). \quad (1.6)$$

- Simple combinations yield

$$\vec{v}_n = \frac{\nu_{in} \vec{V}_n + \nu_{ni} \vec{V}_i}{\nu_{in} + \nu_{ni}} + \frac{(\vec{V}_n - \vec{V}_i) \nu_{ni}}{\nu_{in} + \nu_{ni}} \cdot \exp[-(\nu_{in} + \nu_{ni})t], \quad (1.7)$$

$$\vec{v}_i = \frac{\nu_{in} \vec{V}_n + \nu_{ni} \vec{V}_i}{\nu_{in} + \nu_{ni}} - \frac{(\vec{V}_n - \vec{V}_i) \nu_{in}}{\nu_{in} + \nu_{ni}} \cdot \exp[-(\nu_{in} + \nu_{ni})t]. \quad (1.8)$$

- The two velocities relax very quickly towards the first term on the RHS. Taking $m_i \sim m_n$, and $\vec{V}_n = 0 \Rightarrow$ the relaxed (**common**) velocity for both species

$$v_c = V_i \frac{\nu_{ni}}{\nu_{in} + \nu_{ni}} = V_i \frac{n_{i0}}{n_{i0} + n_{n0}} \simeq V_i \frac{n_{i0}}{n_{n0}}. \quad (1.9)$$

- If ions start to move due to the electromagnetic force caused by the perturbations, the strong friction results in a common velocity which: **i) is much below the starting velocity of the ion fluid, and ii) is achieved very quickly.**

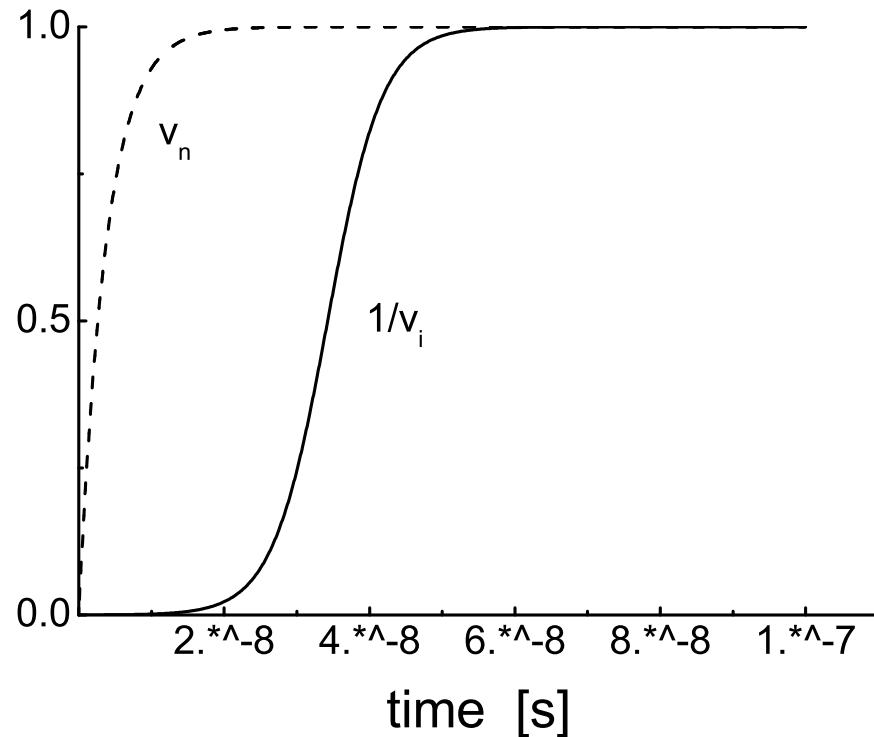


Figure 1.2: The relaxation of the ion and neutral velocities (normalized to $v_c = (\nu_{in}V_n + \nu_{ni}V_i)/(\nu_{in} + \nu_{ni})$) due to collisions, for parameters appropriate for the solar photosphere. The initial velocities for neutrals and ions are respectively 0 and $1.3 \cdot 10^3$ m/s.

- For the same perturbation of the magnetic field (1 percent), we have $v_c = 1.15 \cdot 10^{-4}V_i = 0.15$ m/s. Compare this to the velocity in the ideal case $V_i = 1.3 \cdot 10^3$ m/s. Note also that both V_i and v_c are below/much below the sound velocity

$c_s = 8.9 \cdot 10^3$ m/s, respectively. Hence, neglecting the pressure (compressibility) effects is justified.

- The velocities of both neutrals and ions relax towards the same (normalized) value (= 1) within a time interval which is many orders of magnitude shorter than the wave oscillation period. As a result we have the flux in the weakly ionized plasma (for $m_i = m_p$) given by

$$F = \frac{1}{2}(m_i n_i + m_n n_n) c_A v_c^2 = F_{id} \left(\frac{m_i n_i}{m_i n_i + m_n n_n} \right)^{3/2}. \quad (1.10)$$

- For the given parameters in the photosphere this gives

$$F \simeq 10^{-6} \cdot F_{id} = 5.3 \cdot 10^{-4} \text{ J}/(\text{m}^2 \text{ s}). \quad (1.11)$$

- Actual flux is always small for any realistic amplitude of perturbations. Regardless of the physical mechanism for eventual excitation of the Alfvén waves in the photosphere, the expected amplitude of the perturbed velocity is such that the energy flux of the waves is about one million time smaller than the one obtained from the models that ignore the effects of collisions and the weak magnetization of plasma species.

- The estimated flux presented above is obtained for $m_i = m_p$. Taking $m_i = 35m_p$ we obtain only $F = 0.02 \text{ J}/(\text{m}^2\text{s})$. Assuming in addition a stronger magnetic perturbation of 10 percents, we obtain $F = 2 \text{ J}/(\text{m}^2\text{s})$ and the common velocity amplitude $v_c \simeq 9 \text{ m/s}$. The actual flux may have larger values, e.g. due to stronger magnetic field perturbations, but the linear wave theory becomes unapplicable.

Discussion

- I. Standard estimates of the wave energy flux through the solar photosphere assume a plasma velocity in the photosphere of the order of 1 km/s. This implies two effects. First, that plasma particles move with the observed speed of the convective motion, and, second, that the motion of plasma species involves the magnetic field perturbations due to frozen-in magnetic field effect. The first effect is only partly satisfied. If in the equilibrium neutrals move perpendicular to the magnetic field, say in the x -direction, the plasma particles will move also due to the friction effect.
- The ion drag velocity (in the x -direction) and the drift component (in the y -direction) become, respectively,

$$v_{i0,drag} = v_{ix0} = \frac{1}{1 + \Omega_i^2/\nu_{in}^2} v_{nx0}, \quad (1.12)$$

$$v_{i0,drift} = v_{iy0} = -\frac{\nu_{in}}{\Omega_i} \frac{v_{nx0}}{1 + \nu_{in}^2/\Omega_i^2} = -\frac{\Omega_i}{\nu_{in}} v_{i0,drag}. \quad (1.13)$$

- The corresponding electron components are

$$v_{e0,drag} = v_{ex0} = \alpha_e v_{nx0} \frac{\nu_e}{\Omega_e} \left[\frac{\nu_{en}}{\Omega_e} + \frac{\nu_{ei}}{\Omega_e} \left(1 + \frac{\Omega_e \Omega_i}{\nu_e \nu_{in}} \right) \left(1 + \frac{\Omega_i^2}{\nu_{in}^2} \right)^{-1} \right], \quad (1.14)$$

and

$$v_{e0,drift} = v_{ey0} = \alpha_e v_{nx0} \frac{\nu_{en}}{\Omega_e} \left[1 + \frac{\nu_{ei}}{\nu_{en}} \left(1 - \frac{\Omega_i \nu_e}{\Omega_e \nu_{in}} \right) \left(1 + \frac{\Omega_i^2}{\nu_{in}^2} \right)^{-1} \right]. \quad (1.15)$$

$$\alpha_{e,i} = \frac{1}{1 + \nu_{e,in}^2 / \Omega_{e,i}^2}, \quad \nu_e = \nu_{ei} + \nu_{en}.$$

- The induced ion and electron velocities are not necessarily equal, implying the presence of equilibrium currents. For the same parameters used in Table 1 and taking the neutral velocity of 500 m/s, at $h = 250$ km we have the drag and drift velocities for electrons 315 and 240 m/s, respectively. The ion drag velocity is almost equal to the neutral velocity. This all is due to the fact that

the plasma particles are un-magnetized, $\Omega_i/\nu_i = 3.6 \cdot 10^{-3}$, $\Omega_e/\nu_e = 0.76$. However, due to the same reason the frozen-in condition is far from reality and the ion/electron motion perpendicular to the magnetic lines does not necessarily involve the appropriate movement of the magnetic lines. The actual motions develop as described in the previous section.

II. In view of the known theory⁷, an upwards propagating wave is very weakly damped in the photosphere (the damping is proportional to $1/\nu_{in}$). This holds provided that the wavelengths exceed a certain minimal value. However, it will in fact be more strongly damped in the upper layers, e.g., in the chromosphere where the amount of neutrals decreases but the damping is proportional to ν_{in} .

- Example, assuming the wave propagating towards the chromosphere, the dispersion equation is solved for several wavelengths λ , with all collision frequencies included⁸, at the altitude $h = 1065$ km where $T = 6040$ K, $n_{n0} = 1.71 \cdot 10^{19} /m^3$, $n_0 = 9.35 \cdot 10^{16} /m^3$, and at the altitude $h = 1990$ km where $T = 7160$ K, $n_{n0} = 10^{17} /m^3$, $n_0 = 3.9 \cdot 10^{16} /m^3$.

⁷R. Kulsrud and W. P. Pierce, *Astrophys. J.* **156**, 445 (1969)

⁸J. E. Vernazza, E. H. Avrett, and R. Loeser, *Astrophys. J. Suppl.* **45**, 635 (1981)

Tabel 1.1: Parameters of waves propagating through the chromosphere for two different altitudes.

$h = 1065$ [km]				$h = 1990$ [km]			
λ [km]	ω	kc_a	ω_i/ω_r	λ [km]	ω	kc_a	ω_i/ω_r
0.1	$311 - 1222i$	44855	3.9	0.1	$69666 - 732i$	69829	0.01
1	$327 - 45i$	4485	0.14	1	$6891 - 722i$	6983	0.1
10	$33.1 - 0.45i$	448.5	0.014	10	$371 - 94.5i$	698.3	0.25
100	$3.3 - 0.0045i$	44.85	0.0014	100	$36.4 - 0.9i$	69.8	0.025
500	$0.66 - 0.0002i$	8.97	0.0003	500	$7.3 - 0.04i$	14	0.005

- Shorter wavelengths are more damped at lower altitudes. In the same time, longer wavelengths (i.e., those that are presumably better transmitted by the photosphere) are in fact more damped at higher altitudes. However, this trend certainly can not continue because neutrals vanish at still higher altitudes.
- We stress that the equilibrium parameters change with the altitude and for the large wavelengths the model becomes violated. A numerical approach should give more reliable results.

- Resume:

- The ions and electrons in the photosphere are both un-magnetized, collision frequency with neutrals much larger than the gyro-frequency. **Alfvén-type perturbations involve the neutrals.** The consequences: **i)** In the presence of perturbations the whole fluid (plasma + neutrals) moves; **ii)** The Alfvén velocity includes the total (plasma + neutrals) density \Rightarrow considerably smaller compared to the collision-less case; **iii)** The perturbed velocity of a unit volume, which includes both plasma and neutrals, much smaller compared to the ideal case; **iv)** The wave energy flux through the photosphere becomes orders of magnitude smaller, compared to the ideal case, when the effects of partial ionization and collisions are taken into account consistently.

- More details in:

- Vranjes, Poedts and Pandey, Phys. Rev. Lett. **98**, 049501 (2007)
 - Vranjes et al., Energy flux of Alfvén waves in weakly ionized plasma, Astron. Astrophys. submitted 2007
-

Drift-Alfvén wave

- Magnetic field in the z -direction, $B_0\vec{e}_z$, and an equilibrium plasma density that has a gradient in the perpendicular direction. Low-frequency perturbations $\partial/\partial t \ll \Omega_i$.
- The momentum equations for ions and electrons are

$$m_i n_i \left[\frac{\partial \vec{v}_i}{\partial t} + (\vec{v}_i \cdot \nabla) \vec{v}_i \right] = e n_i \left(-\nabla \phi - \frac{\partial A_z}{\partial t} \vec{e}_z + \vec{v}_i \times \vec{B} \right) - \kappa T_i \nabla n_i - \nabla \cdot \Pi_i - m_i n_i \nu_i \vec{v}_i, \quad (1.16)$$

$$m_e n_e \left[\frac{\partial \vec{v}_e}{\partial t} + (\vec{v}_e \cdot \nabla) \vec{v}_e \right] = -e n_i \left(-\nabla \phi - \frac{\partial A_z}{\partial t} \vec{e}_z + \vec{v}_e \times \vec{B} \right) - \kappa T_e \nabla n_e - \nabla \cdot \Pi_e - m_e n_e (\nu_e \vec{v}_e - \nu_{ei} \vec{v}_i). \quad (1.17)$$

- The parallel electron dynamics described by

$$\left(\frac{\partial}{\partial t} + \vec{v}_{e0} \nabla_{\perp} \right) A_{z1} + \frac{\partial \phi_1}{\partial z} - \frac{\kappa T_e}{n_{e0} e} \frac{\partial n_{e1}}{\partial z} - \frac{m_e \nu_e}{\mu_0 e^2 n_{e0}} \nabla_{\perp}^2 A_{z1} = 0. \quad (1.18)$$

v_{e0} - the equilibrium electron diamagnetic drift velocity; Ampère law used $\nabla \times \vec{B} = \mu_0 \vec{j}$ yielding $en_{e0}\mu_0 v_{ez1} = \nabla_{\perp}^2 A_{z1}$.

- The electron continuity becomes

$$\frac{\partial n_{e1}}{\partial t} + \frac{1}{B_0} (\vec{e}_z \times \nabla_{\perp} \phi_1) \cdot \nabla_{\perp} n_{e0} + \frac{1}{\mu_0 e} \frac{\partial}{\partial z} \nabla_{\perp}^2 A_{z1} = 0. \quad (1.19)$$

- The ion perpendicular motion described by the recurrent formula

$$\begin{aligned} v_{i\perp} = \alpha_i \left[\frac{1}{B_0} \vec{e}_z \times \nabla_{\perp} \phi + \frac{v_{Ti}^2}{\Omega_i} \vec{e}_z \times \frac{\nabla_{\perp} n_i}{n_i} - \frac{\nu_i}{\Omega_i} \frac{\nabla_{\perp} \phi}{B_0} \right. \\ \left. - \frac{\nu_i v_{Ti}^2}{\Omega_i^2} \frac{\nabla_{\perp} n_i}{n_i} + \vec{e}_z \times \frac{\nabla_{\perp} \cdot \Pi_i}{m_i n_i \Omega_i} + \frac{1}{\Omega_i} \left(\frac{\partial}{\partial t} + \vec{v}_{i\perp} \cdot \nabla_{\perp} \right) \vec{e}_z \times \vec{v}_{i\perp} \right. \\ \left. - \frac{\nu_i}{\Omega_i} \frac{\nabla_{\perp} \cdot \Pi_i}{en_i B_0} - \frac{1}{\Omega_i \Omega_i} \left(\frac{\partial}{\partial t} + \vec{v}_{i\perp} \cdot \nabla_{\perp} \right) \vec{v}_{i\perp} \right]. \quad (1.20) \end{aligned}$$

Here $\alpha_i = 1/(1 + \nu_i^2/\Omega_i^2)$.

- Eq. (1.20) is used in the ion continuity equation to calculate the terms $\nabla_{\perp} \cdot (n_i \vec{v}_{i\perp})$. The procedure is straightforward except for the term with the convective derivative in the polarization drift \vec{v}_p , i.e., $(\vec{v}_{i\perp} \cdot \nabla_{\perp}) \vec{e}_z \times \vec{v}_{i\perp}$, and the stress tensor contribution \vec{v}_{π} . For a small equilibrium density gradient, the last $\vec{v}_{i\perp}$ in \vec{v}_p from (1.20) comprises only the leading order perturbed $\vec{E} \times \vec{B}$ and diamagnetic drifts (\vec{v}_{E1} and \vec{v}_{*i1}), while the first \vec{v}_i is the equilibrium ion diamagnetic drift $\vec{v}_{i0} = \kappa T_i \vec{e}_z \times \nabla_{\perp} n_{i0} / (e B_0 n_{i0}) = -\vec{v}_{e0} T_i / T_e$. On the other hand, the stress tensor part after a few steps yields

$$\begin{aligned} \nabla_{\perp} \cdot (n \vec{v}_{\pi}) &= -\rho_i^2 \nabla_{\perp} n_{i0} \cdot \nabla_{\perp}^2 \vec{v}_{i\perp} - n_{i0} \rho_i^2 \nabla_{\perp}^2 \nabla_{\perp} \cdot \vec{v}_{i\perp} \\ &= -\rho_i^2 \nabla_{\perp} n_{i0} \cdot \nabla_{\perp}^2 \vec{v}_{i\perp} + \frac{\rho_i^2 n_{i0}}{\Omega_i} \frac{\partial}{\partial t} \nabla_{\perp}^4 \left(\frac{\phi_1}{B_0} + \frac{v_{Ti}^2 n_{i1}}{\Omega_i n_{i0}} \right). \end{aligned} \quad (1.21)$$

The first term in this expression, within the second order approximation limit, **cancels out** with the term $(\vec{v}_{i0} \cdot \nabla_{\perp}) \vec{e}_z \times \vec{v}_{i\perp}$ from the above discussed convective derivative in the polarization drift which appears in $\nabla_{\perp} \cdot (n_i \vec{v}_p)$. The second term in Eq. (1.21) is the FLR contribution.

- Another similar FLR term is obtained from the time derivative part of $\nabla_{\perp} \cdot (n_i \vec{v}_p)$

reading

$$-n_{i0}\rho_i^2\frac{\partial}{\partial t}\nabla_{\perp}^2\frac{e\phi_1}{\kappa T_i} - \rho_i^2\frac{\partial}{\partial t}\nabla_{\perp}^2 n_{i1}, \quad \rho_i = v_{Ti}/\Omega_i, \quad v_{Ti}^2 = \kappa T_i/m_i. \quad (1.22)$$

• The ion continuity equation finally yields

$$\begin{aligned} \frac{\partial}{\partial t}\left(\frac{n_{i1}}{n_{i0}}\right) + \frac{1}{B_0}\vec{e}_z \times \nabla_{\perp}\phi_1 \cdot \frac{\nabla_{\perp}n_{i0}}{n_{i0}} - \nu_i n_{i0}\rho_i^2\nabla_{\perp}^2\left(\frac{e\phi_1}{\kappa T_i} + \frac{n_{i1}}{n_{i0}}\right) \\ - n_{i0}\rho_i^2\frac{\partial}{\partial t}\nabla_{\perp}^2\left(\frac{e\phi_1}{\kappa T_i} + \frac{n_{i1}}{n_{i0}}\right) + \frac{\rho_i^2 n_{i0}}{\Omega_i}\frac{\partial}{\partial t}\nabla_{\perp}^4\left(\frac{\phi_1}{B_0} + \frac{v_{Ti}^2 n_{i1}}{\Omega_i n_{i0}}\right) = 0. \end{aligned} \quad (1.23)$$

• The two continuity equations combined using the quasi-neutrality

$$\begin{aligned} \left(\frac{\partial}{\partial t} + \nu_i\right)\nabla_{\perp}^2\phi_1 + c_a^2\frac{\partial}{\partial z}\nabla_{\perp}^2 A_{z1} + \frac{\kappa T_i}{en_0}\left(\frac{\partial}{\partial t} + \nu_i\right)\nabla_{\perp}^2 n_1 \\ - \rho_i^2\frac{\partial}{\partial t}\nabla_{\perp}^4\left(\phi_1 + \frac{\kappa T_i}{en_0}n_1\right) = 0. \end{aligned} \quad (1.24)$$

The given set of equations (1.18), (1.19), and (1.24) will be used in the description of the drift-Alfvén waves in collisional plasmas with hot ions.

Waves in unlimited plasma

- In Cartesian geometry, for perturbations $\sim \exp(-i\omega t + ik_y y + ik_z z)$:

$$\begin{aligned}
 & \omega^3 - \omega^2 \left[\omega_{*e} + \omega_{*i} - i \left(\delta + \frac{\nu_i}{1 + k_y^2 \rho_i^2} \right) \right] \\
 & + \omega \left\{ \omega_{*e} \omega_{*i} - \frac{k_z^2 c_a^2}{1 + k_y^2 \rho_i^2} - k_y^2 k_z^2 c_a^2 (\rho_s^2 + \rho_i^2) - \frac{\nu_i \delta}{1 + k_y^2 \rho_i^2} \right. \\
 & \quad \left. - i \left[\omega_{*i} \delta + \frac{\nu_i (\omega_{*e} + \omega_{*i})}{1 + k_y^2 \rho_i^2} \right] + \frac{\omega_{*e} k_z^2 c_a^2}{1 + k_y^2 \rho_i^2} + \frac{\omega_{*i} \nu_i \delta}{1 + k_y^2 \rho_i^2} \right\} \\
 & + i \frac{\nu_i}{1 + k_y^2 \rho_i^2} \left[\omega_{*e} \omega_{*i} - k_z^2 c_a^2 k_y^2 (\rho_s^2 + \rho_i^2) \right] = 0. \tag{1.25}
 \end{aligned}$$

Here, $\omega_{*e} = k_y v_{e0}$, $v_{e0} = -\kappa T_e \kappa_0 / (e B_0)$, $\kappa_0 = n'_0 / n_0$, $\omega_{*i} = k_y v_{i0}$, $v_{i0} = \kappa T_i \kappa_0 / (e B_0)$, $\delta = m_e \nu_e k_y^2 / (\mu_0 n_0 e^2)$.

- In the collision-less limit and for $T_e > T_i$, and after the expansion $(1 + k_y^2 \rho_i^2)^{-1} \simeq 1 - k_y^2 \rho_i^2$, Eq. (1.25) yields the drift-Alfvén mode derived earlier by using the kinetic

theory⁹

$$\omega^3 - \omega^2(\omega_{*e} + \omega_{*i}) - \omega[k_z^2 c_a^2 - \omega_{*e}\omega_{*i} + k_z^2 c_a^2 k_y^2 \rho_s^2] + k_z^2 c_a^2(\omega_{*e} + k_y^2 \rho_s^2 \omega_{*i}) = 0.$$

- In the limit of small $k_y \rho_s$ it reduces to

$$(\omega - \omega_{*e})[\omega^2 - \omega\omega_{*i} - k_z^2 c_a^2] = 0,$$

⇒ the electrostatic drift wave and accelerated and retarded Alfvén waves:

$$\omega_1 = \omega_{*e}, \quad \omega_{2,3} = \frac{1}{2} \left[\omega_{*i} \pm \omega_{*i} \left(1 + \frac{4k_z^2 c_a^2}{\omega_{*i}^2} \right)^{1/2} \right]. \quad (1.26)$$

- For small k_z the two latter waves become¹⁰

$$\omega_2 \simeq \omega_{*i} \equiv -\frac{\omega_{*e} T_i}{T_e}, \quad \omega_3 = \frac{k_z^2 c_a^2}{|\omega_{*i}|}. \quad (1.27)$$

⁹J. Weiland, Collective Modes in Inhomogeneous Plasmas (Institute of Physics Pub., Bristol), 2000

¹⁰ N. A. Krall and A. W. Trivelpiece, Principles of Plasma Physics (McGraw-Hill Kogakusha, Tokyo, 1973), p. 212

Hence, the actual frequencies of the modes in a hot plasma with density gradients in the direction perpendicular to the magnetic field lines, may become very different from the frequencies of the standard Alfvén modes propagating in opposite directions, i.e. $\pm k_z c_a$. This fact should be taken into account in fitting observations into the modeling of solar coronal plasmas.

- In the limit of negligible ion thermal effects

$$\omega^3 - \omega^2 \omega_* - \omega k_z^2 c_a^2 (1 + k_y^2 \rho_s^2) + \omega_* k_z^2 c_a^2 + i \nu_e k_y^2 \lambda_e^2 \omega^2 = 0. \quad (1.28)$$

- in the absence of a density gradient this yields a **damped kinetic-Alfvén mode** (Vranjes et al., Planet. Space Sci. **54**, 641 (2006)).
- in the limit $\omega^2 \ll k_z^2 c_a^2$ we have a standard unstable drift mode (Vranjes and Poedts, Phys. Lett. A **348**, 346 (2006) with frequency $\omega_r = \omega_{*e} / (1 + k_y^2 \rho_s^2)$ and **increment** $\omega_i = \nu_e \omega_{*e}^2 k_y^2 \rho_s^2 / (k_z^2 v_{Te}^2)$. The instability: a common effect of the electron collisions ν_e , the finite ion mass effect (the term $k_y^2 \rho_s^2$), and the equilibrium density gradient (the term ω_{*e}).
- the two modes are **coupled even without collisions**, when $(\omega - \omega_{*e})(\omega^2 - k_z^2 c_a^2) = \omega k_z^2 c_a^2 k_y^2 \rho_s^2$; the coupling vanishes in the limit of negligible $k_y^2 \rho_s^2$, i.e., for the case

of the drift and the non-dispersive Alfvén modes.

- in order to have an electromagnetic drift-Alfvén mode distinguishable from the ion sound mode, the scales along the magnetic field should be much larger compared to those in the perpendicular direction. Hence, to have a reasonable coupling between the drift and kinetic-Alfvén part, and negligible parallel ion dynamics, $k_y \rho_s$ should not be too small, and the parallel wave-length must satisfy¹¹

$$\lambda_z > \frac{2\pi}{k_y \rho_s} L_n, \quad (1.29)$$

otherwise, we would in principle have a threshold for the instability of the drift mode, viz. $\omega_r > k_z c_s$. Here, L_n is the characteristic scale length for the inhomogeneous density. The condition (1.29) can be satisfied even under laboratory conditions and especially in the present solar plasma case with very large vertical scales. In the same time, the omitted electron inertia effects imply $v_{Te} > c_a$, which is equivalent to the plasma $\beta > m_e/m_i$ and to the limit which requires the inclusion of electromagnetic effects¹².

¹¹R. J. Goldston and P.H. Rutherford, Introduction to Plasma Physics, (Institute of Physics Pub., Bristol, 1995), p. 376

¹²J. Weiland, Collective Modes in Inhomogeneous Plasmas (Institute of Physics Pub., Bristol, 2000)

- The character of the solutions may be understood even without directly solving the dispersion equations, by using the generalized Hurwitz method for a general polynomial of the degree m and with complex coefficients¹³:

$$x^m + (a_1 + ib_1)x^{m-1} + \dots + (a_m + ib_m) = 0,$$

Construct the sequence of $m + 1$ numbers $c_0 = 1, c_1 = a_1, \dots, c_r, \dots$, where r goes to m , and where

$$c_r = (-1)^{r(r-1)/2} \begin{vmatrix} a_1 & 1 & 0 & 0 & 0 & \cdot \\ -b_2 & -b_1 & a_1 & 1 & 0 & \cdot \\ a_3 & a_2 & b_2 & b_1 & a_1 & \cdot \\ -b_4 & -b_3 & a_3 & a_2 & -b_2 & \cdot \\ a_5 & a_4 & b_4 & b_3 & a_3 & \cdot \\ \cdot & \cdot & \cdot & \cdot & \cdot & \cdot \\ \cdot & \cdot & \cdot & \cdot & \cdot & \cdot \\ a_{2r-1} & a_{2r-2} & b_{2r-2} & b_{2r-3} & a_{2r-3} & \cdot \end{vmatrix}.$$

- The number of roots with positive real parts equals the number of sign changes in the

¹³ D. L. Giaretta, *Astron. Astrophys.*, **75**, 237 (1979)

sequence c_j . A **sufficient instability condition** is that any of the c_r has a negative sign. As a simple check, we apply the method on Eq. (1.28). Here, we find $c_0 = 1$, $c_1 = -\omega_*$, $c_2 = -\omega_*^2 k_z^2 k_y^2 c_a^2 \rho_s^2 < 0$, $c_3 = c_a^4 k_z^4 \omega_*^3 (\delta^2 + c_a^2 k_y^4 k_z^2 \rho_s^4) > 0$. Consequently, we have two sign changes in the sequence c_j , i.e., two positive real roots, and c_1 and c_2 are both negative, therefore, there exists at least one unstable mode.

Application to solar corona

- Full d.e. solved numerically by taking parameters typical for the quiet inner solar corona, viz. $T_e = T_i = 1.5 \cdot 10^6$ K, $n_{e0} = n_{i0} = 10^{14} \text{ m}^{-3}$, and taking $B_0 = 10^{-3}$ T. Neutrals absent, the dominant collisions between electrons and ions, $\nu_{ei} \simeq 2.1$ Hz, $\nu_{ii} \simeq 0.07$ Hz, $c_s = 1.11 \cdot 10^5$ m/s, $c_a = 2.18 \cdot 10^6$ m/s, $v_{Te} = 4.77 \cdot 10^6$ m/s, $\beta = 0.0052 > m_e/m_i = 0.00054$.
- The behavior of the modes in terms of the parallel wave-number k_z is presented in Fig. 1.3 for $L_n = 10^3$ m and $\lambda_y = 50$ m, while $k_y \rho_s = 0.15$. We thus have a situation similar to that described by Eq. (1.26), i.e., two (retarded and accelerated) damped kinetic-Alfvén modes, lines a and b , respectively, and an electrostatic drift mode (line c). The increment of the drift mode (multiplied by 10^3) is presented by line

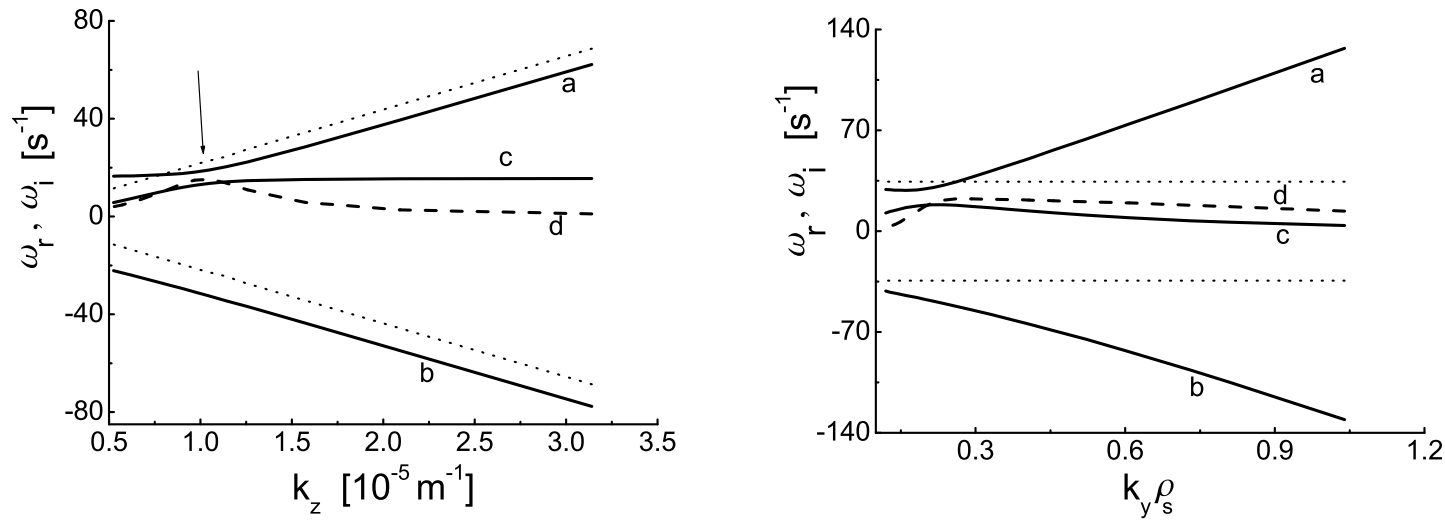


Figure 1.3: Left: frequencies ω_r and increment ω_i of electromagnetic the drift-Alfvén perturbations with the effect of the coupling between the Alfvén (lines *a* and *b*) and drift (line *c*) parts. Dotted lines denote $\pm k_z c_a$. The increment of the electrostatic drift mode (multiplied by 10^3) has a maximum in the region where the retarded kinetic-Alfvén mode and the drift mode change their identities (denoted by arrow). Right: Frequencies ω_r and increment ω_i of the drift-Alfvén perturbations in terms of the coupling term $k_y \rho_s$. The drift wave increment (line *d*) is multiplied by 10^3 . Dotted lines denote $|k_z c_a| = 34.3$ Hz.

d. The drift mode is unstable in the whole range of wave-numbers. Its frequency is nearly constant for large values of k_z . In the area denoted by the arrow, the retarded kinetic-Alfvén mode and the drift mode do not cross each other. Instead, they change identities as typical for an ‘avoided crossing’. For observations, the low frequency (small k_z) domain is of particular importance as this parameter can be measured, i.e.

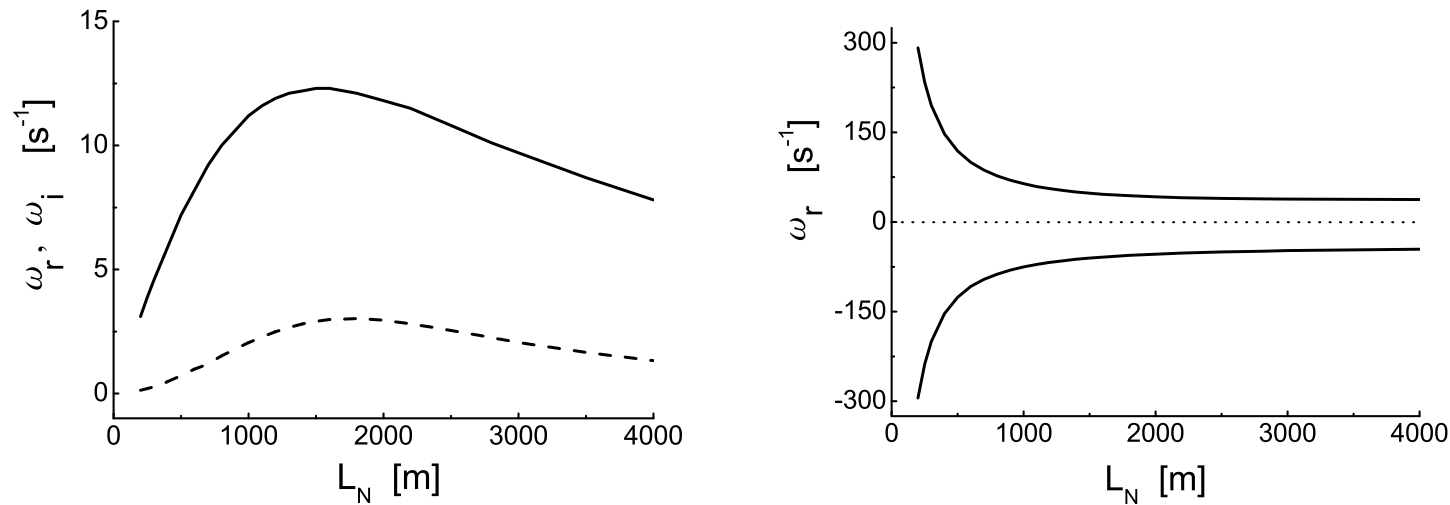


Figure 1.4: Left: the drift wave frequency (full line), and its increment multiplied by 100 (dashed line) in terms of the density scale-length, corresponding to the Alfvén modes (right). Right: the frequency of the kinetic-Alfvén modes corresponding to the drift mode (left), for the given coupling parameter $k_y \rho_s = 0.52$ and $k_z c_a = 34.3$ Hz, in terms of the density scale length.

spatially resolved. It is clearly seen in Fig. 1.3 that, in fact, this is the domain in which the Alfvén mode frequency can be very different from what is expected or predicted if the small-scale plasma inhomogeneity, which drives the drift mode, is neglected. Here, for the given density scale length, the two frequency limits at $k_z \rightarrow 0$ are ± 16.26 Hz. Clearly, the frequencies can be made arbitrary small by changing the equilibrium density scale length L_N .

- The decrement of the Alfvén modes has also been calculated and, in general, the accelerated mode b is less damped. Its damping rate changes between $-3.5 \cdot 10^{-3}$ Hz at $k_z = 3.14$ (in given units), and $-1.1 \cdot 10^{-3}$ Hz at $k_z = 0.5$. The damping rate of the decelerated mode a has a maximum absolute value of about $2.3 \cdot 10^{-2}$ Hz.
- In Fig. 1.3 right we present the mode behavior in terms of the coupling term $k_y \rho_s$ for a fixed value of $|k_z c_a| = 34.3$ Hz (presented by dotted lines). Note that at $k_y \rho_s = 1$ the frequencies of the two kinetic-Alfvén modes are around 127 and -131 Hz. Thus, the actual frequencies may drastically differ from what is expected without the drift mode.
- The drift mode frequency is normally proportional to $1/L_N$. However, due to the coupling with the Alfvén modes, its behavior is also drastically changed. This is seen in Fig. 1.4 where we fix $k_y \rho_s = 0.52$ and $k_z = 400$ km. Here, contrary to what may be expected, for small L_N the mode vanishes and the decrement decreases. This is again due to the identity change with the Alfvén mode. As a matter of fact, the Alfvén frequency for the given numbers is constant $k_z c_a = 34.3$ Hz and the KAWs frequencies (see Fig. 1.4) at large L_N do not change much. For a decreasing L_N the

drift mode curve does not intersect with the Alfvén mode. Instead, the Alfvén mode takes over the behavior of the drift mode: it grows while the drift mode decreases.

- Note that, for the given parameters, the drift curve changes its direction at frequencies around 12 Hz. This is still far enough from the requirement of a small parallel wave-phase velocity in comparison with the electron thermal velocity used in order to omit the electron inertia. Here, we have $k_z v_{Te} = 75$ Hz. Thus, the inclusion of the electron inertia terms is not expected to considerably change the mode behavior.
- A similar sort of identity change of the drift-Alfvén mode, known in the literature (Weiland 2000), happens also in the case when the ion parallel dynamics is retained, and on the condition that $c_a > c_s$. In this case, the sound part of the drift mode is disconnected and the parallel mode dependence goes along the line $k_z c_a$.

Application to solar chromosphere

- Eq. (1.25) is solved also for the quiet Sun parameters of the chromospheric plasma. Here, starting from the altitude of about 2100 – 2200 km and below, the neutral atoms concentration is higher compared to the ions concentration. Within the same range of the parallel wave lengths as in the previous text, the frequencies of the Alfvén modes and the drift mode become below 1 Hz, thus well within the limits of detection. Yet, the ion-neutral collisions appear strong enough to damp all three modes in the given wave length range. However, in this region the parameters change rapidly with the altitude so that it has no sense to consider such long parallel wave lengths. Setting $T = 3.2 \cdot 10^4$ K, and $n_{n0} = n_{i0} = 1.5 \cdot 10^{16} \text{ m}^{-3}$, it turns out that for a short density scale $L_N \simeq 10^2$ m, and for $\lambda_y \simeq 10$ m and $\lambda_z \simeq 10$ km, the drift mode is highly unstable, with a frequency $\omega_r \simeq 16$ Hz and increment $\omega_i \simeq 2$ Hz. Here, $\nu_{in} \simeq 2$ Hz and $\nu_e \simeq 6 \cdot 10^4$ Hz.

Eigen-modes in bounded plasma

- **Global** mode behavior in magnetic structures that are highly elongated along the magnetic field lines and localized in the perpendicular direction.

- Use

$$\nabla_{r,\theta} = \vec{e}_r \frac{\partial}{\partial r} + \frac{\vec{e}_\theta}{r} \frac{\partial}{\partial \theta}, \quad \nabla_{r,\theta}^2 = \frac{\partial^2}{\partial r^2} + \frac{1}{r} \frac{\partial}{\partial r} + \frac{1}{r^2} \frac{\partial^2}{\partial \theta^2},$$

and consider perturbations of the form $\hat{f}(r) \exp(-i\omega t + im\theta + ik_z z)$, where $\hat{f}(r)$ denotes the r -dependent amplitude and m the discrete poloidal mode number. In the same frame we have $\vec{v}_{(e,i)0} = \mp \vec{e}_\theta \kappa T_{e,i} n'_0 / (e B_0 n_0) = v_{(e,i)0}(r) \vec{e}_\theta$, $n'_0 = dn_0/dr$, with the minus sign for electrons.

- The combined electron dynamics equations (1.18) and (1.19) yield:

$$\left(\nabla_{\perp}^2 + \frac{\frac{\omega \omega_2}{c_a^2 k_z^2 \rho_s^2}}{1 - \frac{i\nu_e \omega}{k_z^2 v_{Te}^2}} \right) \hat{A}_{z1} - \frac{1}{k_z c_a^2} \frac{\frac{\omega}{\rho_s^2} + \frac{m \Omega_i n'_0}{r n_0}}{1 - \frac{i\nu_e \omega}{k_z^2 v_{Te}^2}} \hat{\phi}_1 = 0, \quad (1.30)$$

where $\omega_2 = \omega - v_{e0}(r)m/r$, and $\nabla_{\perp}^2 = \partial^2/\partial r^2 + \partial/(r\partial r) - m^2/r^2$.

- The ion part can be discussed in two limits.

Negligible ion thermal effects

- From the combined continuity equations

$$\nabla_{\perp}^2 \hat{\phi}_1 - \frac{k_z^2 c_a^2}{\omega} \nabla_{\perp}^2 \hat{A}_{z1} = 0, \quad (1.31)$$

- To decouple the equations assume $n_0(r) = N_0 \exp(ar^2/2)$, where a can be both positive and negative, and r takes values between 0 and r_0 .

$$\nabla_{\perp}^2 \left\{ \left[\nabla_{\perp}^2 - \frac{\omega/\rho_s^2 + am\Omega_i}{\omega(1-i\delta_1)} + \frac{\omega(\omega + am\kappa T_e/eB_0)}{k_z^2 \rho_s^2 c_a^2 (1-i\delta_1)} \right] \hat{\phi}_1 \right\} = 0. \quad (1.32)$$

or

$$\nabla_{\perp}^2 \psi(r) = 0, \quad (1.33)$$

- Consequently

$$\left[\nabla_{\perp}^2 - \frac{\omega/\rho_s^2 + am\Omega_i}{\omega(1-i\delta_1)} + \frac{\omega(\omega + am\kappa T_e/eB_0)}{k_z^2 \rho_s^2 c_a^2 (1-i\delta_1)} \right] \hat{\phi}_1 = \psi(r), \quad (1.34)$$

and from Eq. (1.33) $\psi(r)$ is

$$\psi(r) = 0, \quad \text{or} \quad \psi(r) = c_1 \cosh[m \log(r)] + c_2 \sinh[m \log(r)]. \quad (1.35)$$

• Eq. (1.34) can be written in the form

$$\left(\frac{\partial^2}{\partial r^2} + \frac{1}{r} \frac{\partial}{\partial r} - \frac{m^2}{r^2} + \xi^2 \right) \left[\hat{\phi}_1 - \frac{\psi(r)}{\xi^2} \right] = 0, \quad (1.36)$$

where

$$\xi^2 = \frac{\omega(\omega + \omega_0)}{\rho_s^2(1 - i\delta)} \left(\frac{1}{c_a^2 k_z^2} - \frac{1}{\omega^2} \right), \quad \omega_0 = am \frac{\kappa T_e}{eB_0}, \quad \delta = \frac{\nu_e \omega}{k_z^2 v_{Te}^2}.$$

• The solutions: the Bessel functions of the first and the second kind, $J_n(\xi r)$ and $Y_n(\xi r)$, with a complex argument. Theorems of Lommel and Bourget¹⁴: if $n > -1$, then the zeros of the Bessel function $J_n(z)$ with the complex argument z are all real, and, for $n \geq 0$ the functions $J_n(z)$ and $J_{n+s}(z)$ have no common zeros other than the origin, for all $s > 0$. Hence, for vanishing solutions at the boundary, we set that $\xi r_0 = \varepsilon_l$ where ε_l is the real l -th zero of the complex function $J_n(\xi r)$.

¹⁴G. N. Watson, A treatise on the Theory of Bessel Functions (Cambridge at the University Press, Cambridge), pp. 482-485 (1962)

- The dispersion equation for the radially bounded plasma

$$\left(\omega + am \frac{\kappa T_e}{e B_0} \right) (\omega^2 - k_z^2 c_a^2) = \omega k_z^2 c_a^2 \frac{\varepsilon_l^2 \rho_s^2}{r_0^2} (1 - i\delta). \quad (1.37)$$

- This is the equivalent to Eq. (1.28) in an unbounded plasma. Both m and ε_l take given discrete values. Eq. (1.37) describes the global drift-Alfvén wave, with an unstable drift wave part. The poloidal (i.e. in the θ -direction) propagation is the consequence of the drift mode which propagates perpendicular to both the magnetic field lines and the density gradient. Combined with the given z -dependence, this gives the twisting of the global modes. The twisting vanishes for $m = 0$ when the two modes decouple. The eigen-functions \hat{A}_{z1} can be easily found from Eq. (1.31), and \hat{n}_1 from Eq. (1.19), which is rewritten as

$$\hat{n}_1 = \frac{k_z}{\mu_0 e \omega} \nabla_{\perp}^2 \hat{A}_{z1} - \frac{m}{r} \frac{n'_0}{\omega B_0} \hat{\phi}_1. \quad (1.38)$$

- Mode details are available in: Vranjes and Poedts, Phys. Plasmas **13**, 032107 (2006).

The hot ion case

- Ion thermal effects enter the equations through (1.22), the second term in (1.21), and the collisions. Using Eq. (1.38) in (1.24) for the same Gaussian/inverse-Gaussian density profile as before, we obtain an equation containing terms proportional to $\rho_i^4 \nabla_{\perp}^4 \hat{\phi}_1$ and $\rho_i^6 \nabla_{\perp}^6 \hat{A}_{z1}$, which come from the second part of the stress tensor in Eq. (1.21). This 6th-order differential equation is to be combined with the 2nd-order Eq. (1.41) in order to decouple the two potentials. In the case of the global modes studied here and, therefore, for large scales, we have $|\rho_i \nabla_{\perp}| < 1$ and the high order derivatives yield small terms that can be neglected. Hence, by omitting the stress tensor contribution while still keeping the ion thermal effects through (1.22) and the collisions, from the combined continuity equations:

$$\nabla_{\perp}^2 \left\{ \hat{\phi}_1 - \frac{k_z c_a^2}{(\omega + i\nu_i)(\omega - m a \rho_i^2 \Omega_i)} \left[\omega - (\omega + i\nu_i) \rho_i^2 \nabla_{\perp}^2 \right] \hat{A}_{z1} \right\} = 0. \quad (1.39)$$

• This gives

$$\hat{\phi}_1 = \frac{k_z^2 c_a^2}{(\omega + i\nu_i)(\omega - m a \rho_i^2 \Omega_i)} \left[\omega - \rho_i^2 (\omega + i\nu_i) \nabla_{\perp}^2 \right] \hat{A}_{z1} + \psi(r), \quad (1.40)$$

which is used in

$$\left(\nabla_{\perp}^2 + \frac{\frac{\omega \omega_2}{c_a^2 k_z^2 \rho_s^2}}{1 - \frac{i\nu_e \omega}{k_z^2 v_{Te}^2}} \right) \hat{A}_{z1} - \frac{1}{k_z c_a^2} \frac{\frac{\omega}{\rho_s^2} + \frac{m \Omega_i n'_0}{r n_0}}{1 - \frac{i\nu_e \omega}{k_z^2 v_{Te}^2}} \hat{\phi}_1 = 0, \quad (1.41)$$

$$\Rightarrow \left(\frac{\partial^2}{\partial r^2} + \frac{1}{r} \frac{\partial}{\partial r} - \frac{m^2}{r^2} + \eta^2 \right) [\hat{A}_{z1} + c\psi(r)] = 0. \quad (1.42)$$

$$\eta^2 = \left[\omega(\omega + i\nu_i) \left(\omega + m a \rho_s^2 \Omega_i \right) \left(\omega - m a \rho_i^2 \Omega_i \right) - \omega k_z^2 c_a^2 \left(\omega + m a \rho_s^2 \Omega_i \right) \right] \left\{ k_z^2 c_a^2 (\omega + i\nu_i) \left[\rho_s^2 (1 - i\delta_1) \left(\omega - m a \rho_i^2 \Omega_i \right) + \rho_i^2 (\omega + m a \rho_s^2 \Omega_i) \right] \right\}^{-1}, \quad c = \frac{(\omega + m a \rho_s^2 \Omega_i)}{k_z c_a^2 \rho_s^2 \eta^2 (1 - i\delta_1)}.$$

- As earlier, the solutions are the Bessel functions of the first kind and the corresponding dispersion equation reads

$$\eta^2 = \frac{\varepsilon_l^2}{r_0^2}. \quad (1.43)$$

- In the cold ion limit, it reproduces Eq. (1.37). The solutions of Eq. (1.43) describe the eigen-values of the global eigen-modes in the given cylindrical plasma. Eq. (1.43) can be easily solved numerically for various harmonics by choosing the appropriate ε_l and m . In the case of solar coronal magnetic structures, the density and the magnetic field have higher values compared to the previous case, $n_{i0} = n_{e0} = 10^{16} \text{ m}^{-3}$ and $B_0 \simeq 10^{-2} \text{ T}$, and the condition (1.29) now can be rewritten as $2\pi / (ma\rho_s\lambda_z) < 1$. Here, we have set $\kappa_0 \equiv n'_0/n_0 \simeq ar_0$. Taking as an example a magnetic column with the diameter of 200 km and, in the case when the density at its edge is 0.1 of its value at the column axis, we get $a \simeq 7 \cdot 10^{-10} \text{ m}^{-2}$, and therefore, the poloidal mode number m takes very high values $\sim 10^5$.

Resume:

- The stability discussed of the drift-Alfvén wave in unbounded and bounded, collisional solar plasmas, including the effects of hot ions and a finite ion Larmor radius. The density gradient + the electron collisions with heavier plasma species \Rightarrow the instability of the electrostatic drift mode which is coupled to the dispersive Alfvén mode.
- The exchange of identity between the electrostatic and electromagnetic modes \Rightarrow the frequency of the electromagnetic part of the mode becomes very different compared to the case without the density gradient.
- In the application to the magnetic structures the complex eigen-modes and the corresponding complex discrete eigen-frequencies in cylindric, radially inhomogeneous, collisional and bounded plasma derived and discussed.
- the dispersion equation involves a **discrete poloidal mode number**, and eigen-functions in terms of Bessel functions with **discrete zeros at the boundary**.
- the problem is doable analytically even if some realistic physical effects (geometry, collisions) are included.

More details in: [Vranjes and Poedts, Astron. Astrophys. **458**, 635 \(2006\).](#)

Additional works on the subject:

- J. Vranjes and S. Poedts, Low frequency waves in bounded streaming plasma, *Phys. Plasmas* **12**, 064501 (2005).
- D. Petrovic, J. Vranjes and S. Poedts, Analysis of waves in strongly collisional photospheric plasma, *Astron. Astrophys.* **461**, 277 (2007).
- H. Saleem, J. Vranjes, and S. Poedts, Unstable drift mode driven by shear plasma flow in solar spicules, accepted to *Astron. Astrophys.* (2007)